sustainability

MDPI

Article

Shear Performance of Optimized-Section Precast Slab with Tapered Cross Section

Hyunjin Ju [1], Sun-Jin Han [2], Hyo-Eun Joo [2], Hae-Chang Cho [2], Kang Su Kim [2,*] and Young-Hun Oh [3]

[1] Department of Civil Engineering and Natural Hazards, University of Natural Resources and Life Sciences, Vienna, Feistmantelstrasse 4, 1180 Vienna, Austria; hyunjin.ju@boku.ac.at

[2] Department of Architectural Engineering, University of Seoul, 163 Siripdaero, Dongdaemun-gu, Seoul 130-743, Korea; sjhan1219@gmail.com (S.-J.H.); joo8766@uos.ac.kr (H.-E.J.); chang41@uos.ac.kr (H.-C.C.)

[3] Department of Medical Space Design & Management, Konyang University, 158 Gwanjeodong-ro, Seo-gu, Daejeon 35365, Korea; youngoh@konyang.ac.kr

* Correspondence: kangkim@uos.ac.kr; Tel.: +82-2-6490-5576

Received: 23 November 2018; Accepted: 22 December 2018; Published: 29 December 2018

Abstract: The optimized-section precast slab (OPS) is a half precast concrete (PC) slab that highlights structural aesthetics while reducing the quantity of materials by means of an efficient cross-sectional configuration considering the distribution of a bending moment. However, since a tapered cross section where the locations of the top and bottom flanges change is formed at the end of the member, stress concentration occurs near the tapered cross section because of the shear force and thus the surrounding region of the tapered cross section may become unintentionally vulnerable. Therefore, in this study, experimental and numerical research was carried out to examine the shear behaviour characteristics and performance of the OPS with a tapered cross section. Shear tests were conducted on a total of eight OPS specimens, with the inclination angle of the tapered cross section, the presence of topping concrete and the amount of shear reinforcement as the main test variables and a reasonable shear-design method for the OPS members was proposed by means of a detailed analysis based on design code and finite-element analysis.

Keywords: optimized section; precast slab; concrete; tapered cross section; shear performance

1. Introduction

The optimized-section precast slab (OPS) is a half precast concrete (PC) slab designed with a cross-sectional shape optimized by locating the top and bottom flanges differently at the centre and end of the member so that they can effectively resist the positive and negative moments [1]. As shown in Figure 1a, the lower section of the OPS has excellent structural aesthetics and thus can improve economic efficiency because there is no need for finishing work. As shown in Figure 1a–e, the concrete compression flange was placed at the upper part in the centre section of the span and the lower part in the end section of the spans so as to efficiently resist the compressive force generated due to the bending moment distribution caused by vertical loads. In addition, the structural performance was improved by introducing prestress into the member. Truss-type shear reinforcement was placed in each rib to improve the composite performance of the OPS and topping concrete as well as vertical shear resistance.

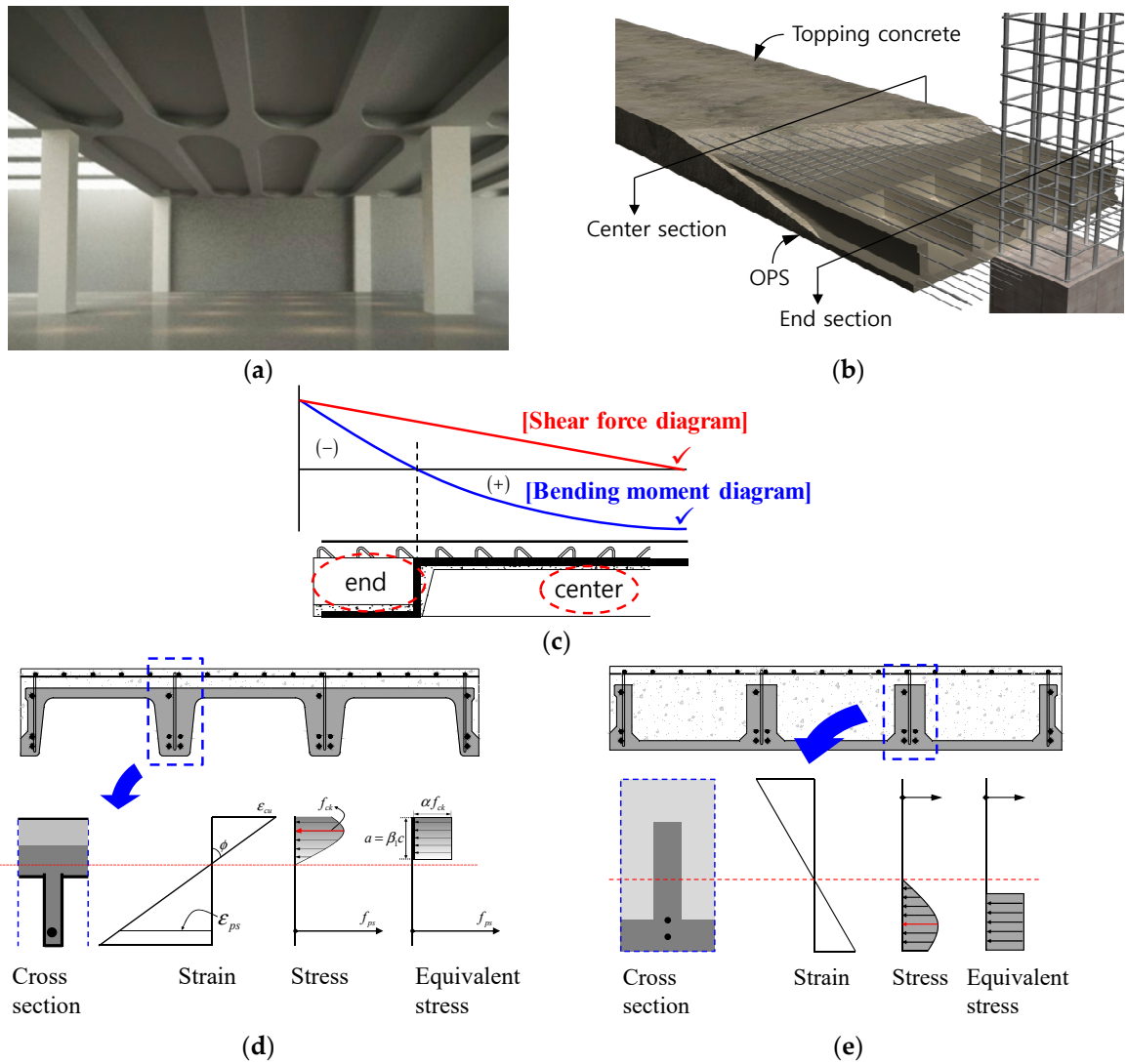

Figure 1. Optimized-section precast slab (OPS). (**a**) Bottom view of OPS system. (**b**) Description of OPS system. (**c**) Location of compression flange. (**d**) Centre section. (**e**) End section.

Nowadays, there is a high demand to reduce carbon emission and eco-friendly construction has become an important issue for sustainability of structures. Among structural members of a building, slabs are known to be heavily responsible for the carbon emission because they cause about 35% of the total carbon emission from structural members [2]. Considering that the PC method, used for producing the OPS members, can minimize waste of materials [3] and that their shapes are optimized by removing unnecessary parts of sections, the OPS members are productions of the sustainable and eco-friendly construction method. In construction markets, it is also very important to secure proper efficiency, constructability and short construction period. The optimized-section precast slabs (OPS) are produced in a precast concrete (PC) factory and assembled on sites. Thus, the OPS system does not require formworks or curing periods that are essential for any conventional reinforced concrete (RC) construction method, which is why it requires a very short construction period. The OPS system can also lead to save materials by adopting the efficient sectional shapes and to reduce manpower by utilizing automatic fabrication facilities [1,4]. On the other hand, it was confirmed that OPS system is more economical about 10% than the conventional RC slab system in a distribution centre and a basement garage construction because of its high load-carrying capacity [3].

According to previous researches [5–7], a large rotation at member ends causes many problems with serviceability such as cracks and large deflection, which depends on support types and joint details. In a fundamental point of view, a flexural member can be more efficiently designed by

utilizing the continuous support conditions because the static moment can be distributed into positive and negative moments resulting in a larger load carrying capacity than a simply supported member. For these reasons, many researches have been conducted on continuous PC members [5–10] and particularly in the authors' previous study [1], the flexural performance of continuous OPS members was studied in detail.

In the previous research [1], critical cracks occur in sections where the sectional area of the concrete is relatively small (i.e., near the tapered section). This is because the tapered cross section is formed where the positions of the top and bottom flanges change because of the characteristics of the OPS member. Since the crack angle is higher than 0.79 rad (45°), the truss bars placed in the ribs may not effectively resist the shear force. In addition, at the tapered section where the section changes drastically, local stress concentration or damage can occur with large shear forces [6], which is influenced by its shape and angle. Therefore, in this study, shear tests on the composite slab with topping concrete and the precast concrete (PC) slab unit were conducted to examine the shear performance of the OPS according to the shape and angle of the tapered cross-section. Numerical research using a finite-element analysis (FEA) and structural design code was also carried out. Furthermore, this study analysed the validity of the current design method in detail and proposed a reasonable shear-design method for OPS members.

2. Test Program

2.1. Details of Test Specimens

In this study, shear tests were planned considering the presence of topping concrete composite and the inclination angle of the tapered cross section as the main variables, as shown in Figure 2 and the amount of shear reinforcement was set as an additional variable in consideration of the spacing of the shear reinforcement for the OPS specimen with topping concrete. Figure 3 shows the section details of the US series specimens, which are PC unit members and CS series specimens, which are composite members with topping concrete. Table 1 summarizes the material properties and reinforcement details for each specimen. A total of four test specimens were fabricated and eight shear test results were obtained from tests conducted on the left and right side sections of each member. The angles of the tapered cross sections were planned to be 0.52 rad (30°), 1.05 rad (60°) and 1.57 rad (90°) for PC unit members and these specimens were named as US30, US60 and US90, respectively. Here, for the US60, tests on specimens with the same details were conducted twice; so the specimens were named US60a and US60b, respectively. For the composite members, the specimens in which the angles of the tapered cross sections were set at 0.52 rad (30°) and 1.57 rad (90°) were named as CS30 and CS90 and the specimens with more shear reinforcement than the CS30 and CS90 specimens were named as CSS30 and CSS90, respectively. As shown in Table 1, the concrete compressive strength of a PC slab unit was 46.9 MPa or 55.0 MPa and the compressive strength of topping concrete was 49.0 MPa. In addition, the yield strengths of D10, D16 and D19 rebars used in the test specimens were 505, 462 and 472 MPa, respectively.

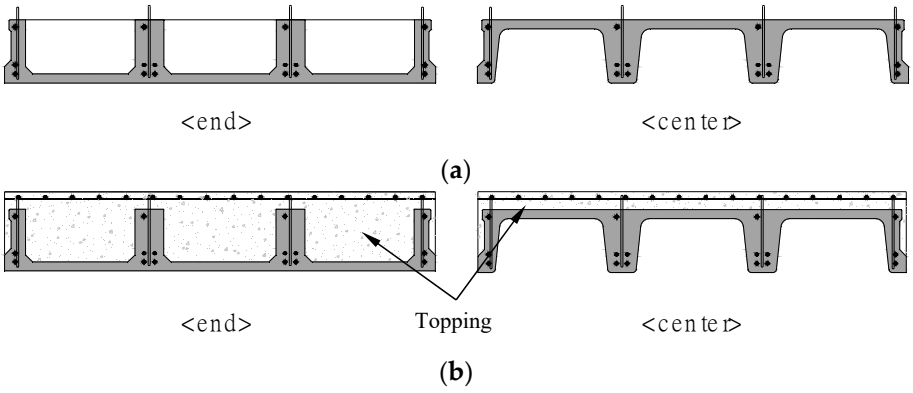

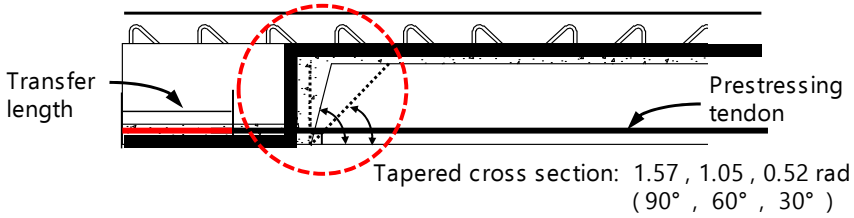

(**c**)

Figure 2. Summarized description of specimens. (**a**) Section of PC slab unit specimens (US series). (**b**) Section of composite slab specimens (CS series). (**c**) Tapered cross section according to inclination angle.

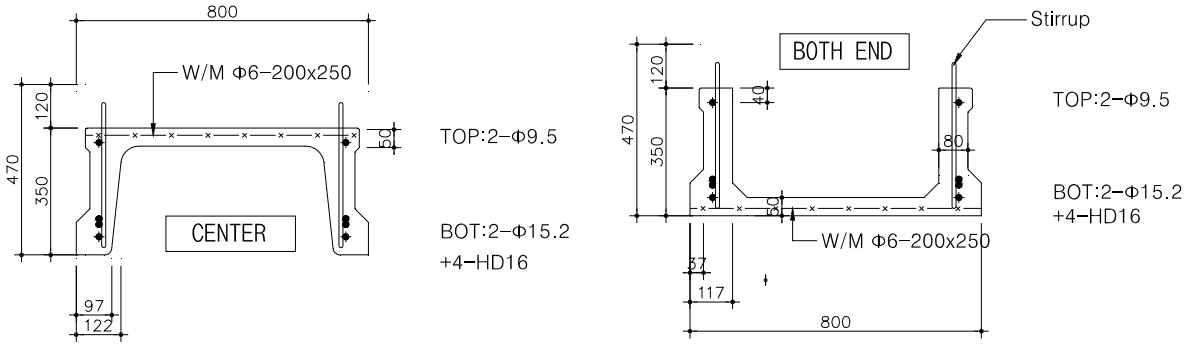

(**a**)

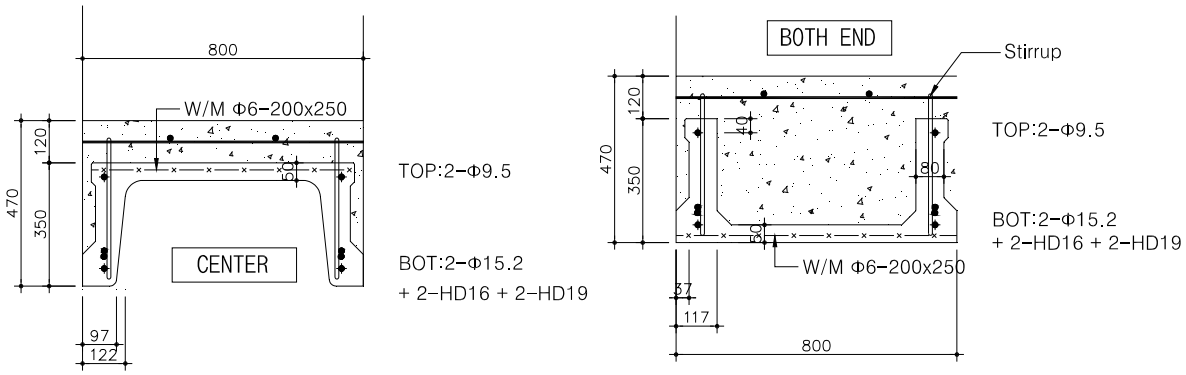

(**b**)

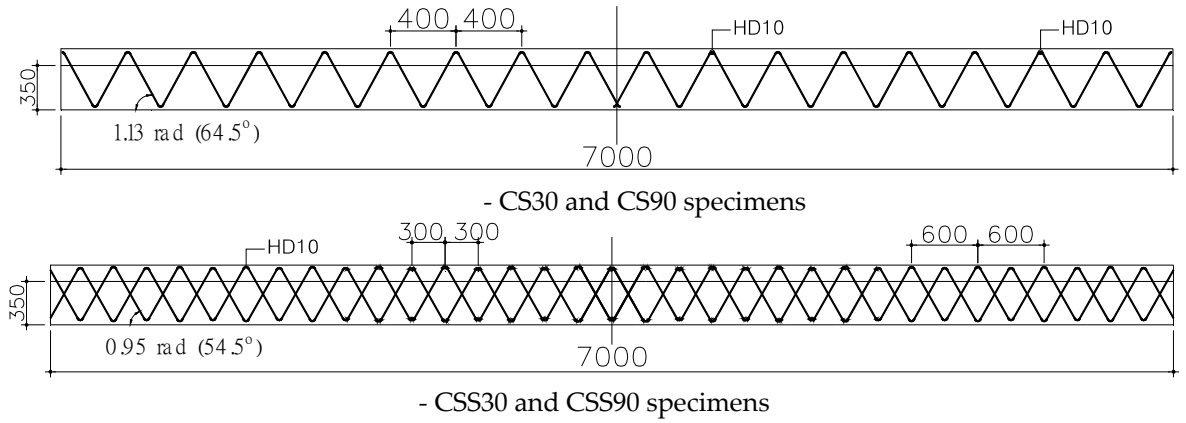

(**c**)

Figure 3. Section details of test specimens (unit: mm and degree). (**a**) US series specimens. (**b**) CS series specimens. (**c**) Shear reinforcement in CS series specimens.

Table 1. Material properties and reinforcement details of specimens (unit: mm and rad).

Specimen	Compressive Strength of Concrete, f_c' (MPa)		Compressive Reinforcement (Sectional Area, mm^2)		Tensile Reinforcement (Sectional Area, mm^2)		Shear Reinforcement	Angle of Inclined Section (rad)
	PC	Topping	Rebar	Tendon	Rebar	Tendon		
US30	55.0	-	-	2-ϕ9.5 (110)	4-D16 (794)	2-ϕ15.2 (280)	D10@400	0.524 (30°)
US60a	46.9	-		2-ϕ9.5 (110)	4-D16 (794)	2-ϕ15.2 (280)	D10@400	1.047 (60°)
US60b	46.9	-		2-ϕ9.5 (110)	4-D16 (794)	2-ϕ15.2 (280)	D10@400	1.047 (60°)
US90	55.0	-	-	2-ϕ9.5 (110)	4-D16 (794)	2-ϕ15.2 (280)	D10@400	1.571 (90°)
CS30	55.0	49.0	2-D10 (143)	2-ϕ9.5 (110)	2-D16 +2-D19 (970)	2-ϕ15.2 (280)	D10@400	0.524 (30°)
CS90	55.0	49.0	2-D10 (143)	2-ϕ9.5 (110)	2-D16 +2-D19 (970)	2-ϕ15.2 (280)	D10@400	1.571 (90°)
CSS30	55.0	49.0	2-D10 (143)	2-ϕ9.5 (110)	2-D16 +2-D19 (970)	2-ϕ15.2 (280)	D10@600 +D10@600	0.524 (30°)
CSS90	55.0	49.0	2-D10 (143)	2-ϕ9.5 (110)	2-D16 +2-D19 (970)	2-ϕ15.2 (280)	D10@600 +D10@600	1.571 (90°)

As shown in Figure 3, the length and width of all specimens were 7 m and 800 mm, respectively. The height of the PC slab unit was 350 mm and that of the topping concrete 120 mm. The 7-wire strands with a tensile strength (f_{pu}) of 1860 MPa were used to produce the PC slab unit and two strands with diameters of 15.2 mm and 9.5 mm were placed at the top and bottom, respectively. The yield stress of strands (f_{py}) determined by using the 0.1% offset method was 1645 MPa and the initial prestress (f_{pi}) introduced in the strands was about 0.7 f_{pu}, which was estimated to be 137.3 kN and 63.8 kN for the 15.2 mm and 9.5 mm strands, respectively, in terms of prestressing forces. For the US specimens, four reinforcing bars with a diameter of 16 mm were additionally placed on the tension side to provide sufficient flexural capacity and induce shear failure. Meanwhile, in the design of the test specimens, the flexural and shear strengths were calculated based on the ACI318-14 code [11]. For the CS specimens with topping concrete, two deformed reinforcing bars with diameters of 16 mm and 19 mm were arranged on the tension side, as shown in Figure 3b. Figure 3c shows the details of the shear reinforcement placed in the CS series specimens. The shear reinforcement was fabricated in the form of a truss by bending D10 deformed bars and placed on each rib during the production of the PC slab unit. The spacing of shear reinforcement placed in the US and CS specimens was 400 mm. In the CSS specimens, two sets of truss bars with 600 mm spacing were placed crosswise, so that shear reinforcement was placed at intervals of 300 mm. The height of the truss bar was 420 mm and the net cover thickness was 25 mm.

2.2. Test and Measurement Setup

Figure 4 shows the loading and measurement setups for test specimens. As shown in Figure 4a, the specimens were simply supported at points installed 50 mm away and 3750 mm away from the end of the member. One-point loading was applied at a point 1200 mm away from the end of the member to induce shear failure near the end section where the tapered cross section is located. The load was applied by a 1000 kN actuator under displacement control and the loading rate was 1.5 mm/min. up to failure. Shear tests were carried out at one end and then at the other, undamaged opposite end. Figure 4b,c shows the inclination angles of the tapered cross sections for the US and CS series specimens, respectively. The US60 specimens with a 1.05 rad (60°) inclination angle have the same details for both ends, whereas the remaining specimens were designed to have inclination angles of 0.52 rad (30°) and 1.57 rad (90°) on the left and right ends, respectively. The deflections of the test specimens were measured using a LVDT installed under the section of the loading point.

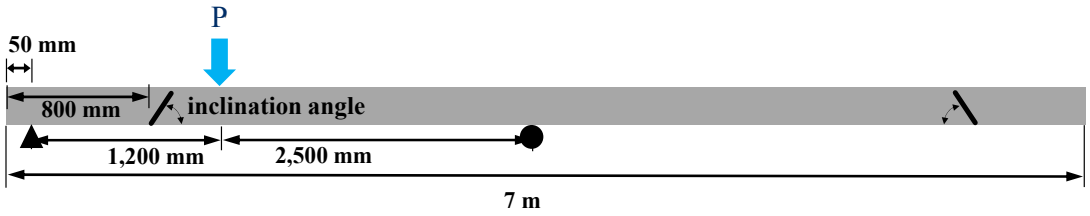

(**a**)

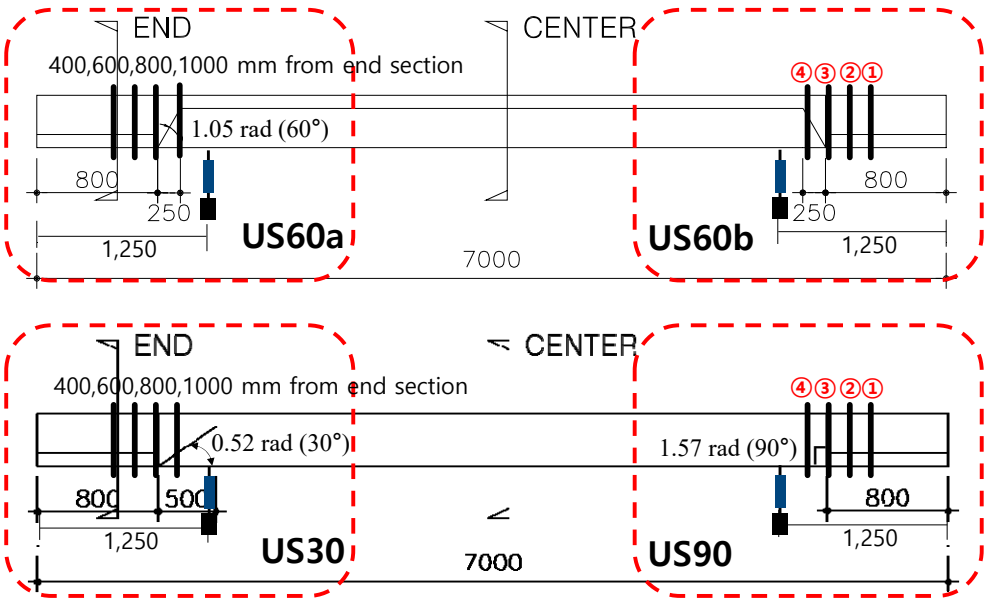

(**b**)

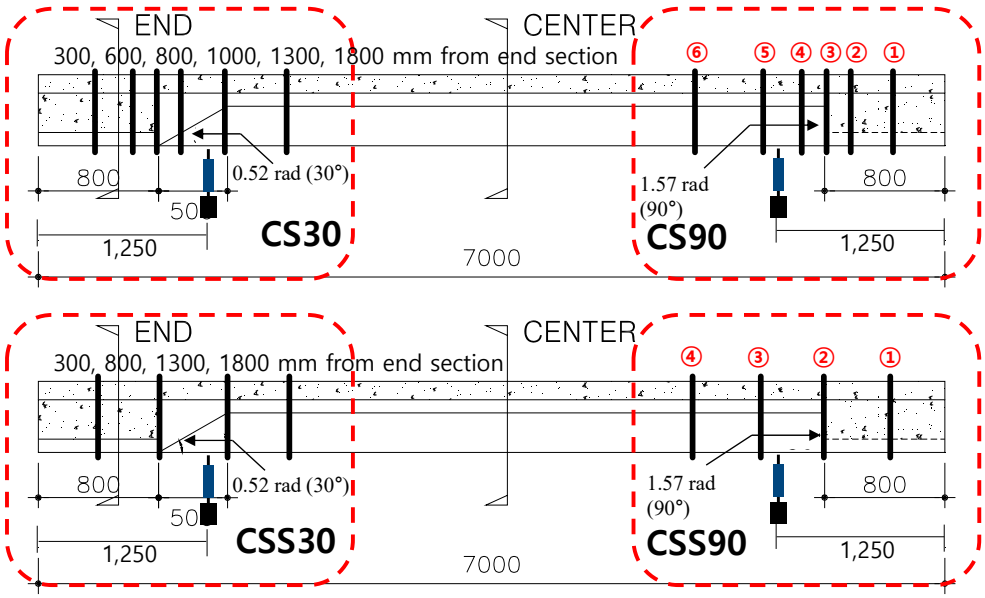

(**c**)

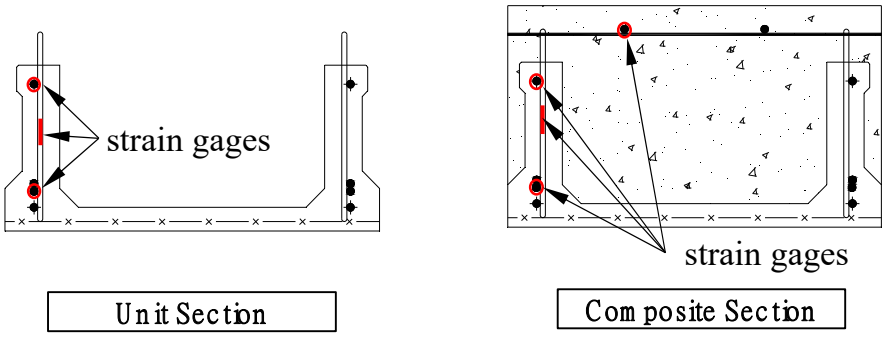

(**d**)

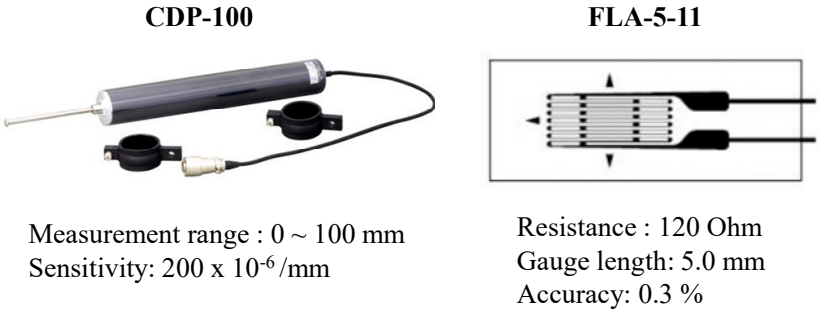

(**e**)

Figure 4. Test and measurement setup. (**a**) Loading setup. (**b**) PC slab unit specimens. (**c**) Composite slab specimens. (**d**) Location of strain gages in section. (**e**) Measurement instruments.

In Figure 4b,c, the thick vertical solid lines indicate the section positions where gauges were installed to measure the strains of longitudinal and shear reinforcements. Figure 4d shows the locations of gauges installed in sections. For the US specimens, strain gauges were installed in the tensile reinforcement, prestressing strands on the compression side and shear reinforcement in sections 400, 600, 800 and 1000 mm away from the end, as shown in the 'unit section' of Figure 4d. For the CS specimens, as shown in the 'composite section' of Figure 4d, strain gauges were installed in the tensile reinforcement, shear reinforcement, prestressing strands on the compression side and

longitudinal reinforcement in the topping concrete at the sections indicated by the thick vertical solid lines in Figure 4c. The details of the instruments used in the test are summarized in Figure 4e.

3. Test Results

3.1. Shear Behaviour and Crack Pattern of Test Specimens

Figure 5 shows the load-deflection curves of the test specimens and Figure 6 shows the crack patterns of the specimens at the shear failure. Among the PC slab unit specimens (US series), the US90 specimen, which had the largest angle of the tapered cross section, showed the lowest maximum load of 169 kN and the remaining specimens exhibited similar maximum loads, ranging from 222 to 248 kN. In addition, the initial cracking loads of the US specimens ranged from 72 to 85 kN. The stiffness decreased after the occurrence of the initial cracks and the US90 specimen showed the greatest reduction in stiffness. The US60a and US60b specimens exhibited relatively ductile behaviour compared to the other US specimens. This is due to the significant contribution of flexural deformations as the ultimate failure modes shown in Figure 6c,d. On the other hand, the US90 specimen showed damage concentrated in the vicinity where the tapered cross section is formed and underwent premature failure as the top flange collapsed. This is because a relatively larger stress concentration occurred as the section was drastically changed due to the larger inclination angle of the tapered cross section.

PC slab unit specimen	US30	US60a	US60b	US90
Maximum load (kN)	225	248	222	169
Composite slab specimen	CS30	CS90	CSS30	CSS90
Maximum load (kN)	394	404	440	441

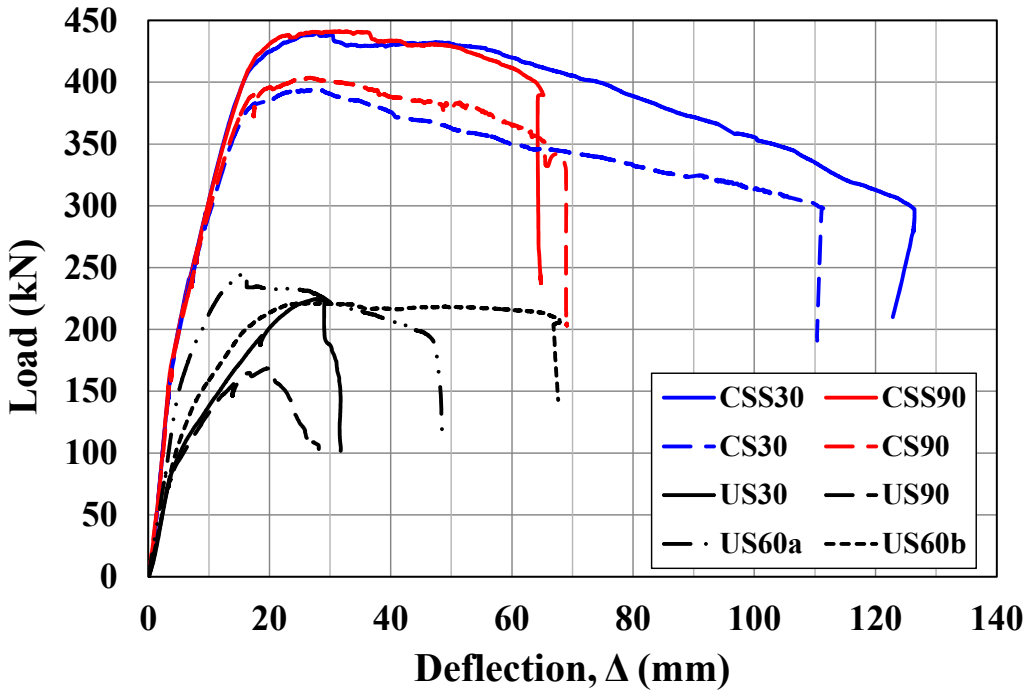

Figure 5. Load-deflection curves.

(**a**) (**b**)

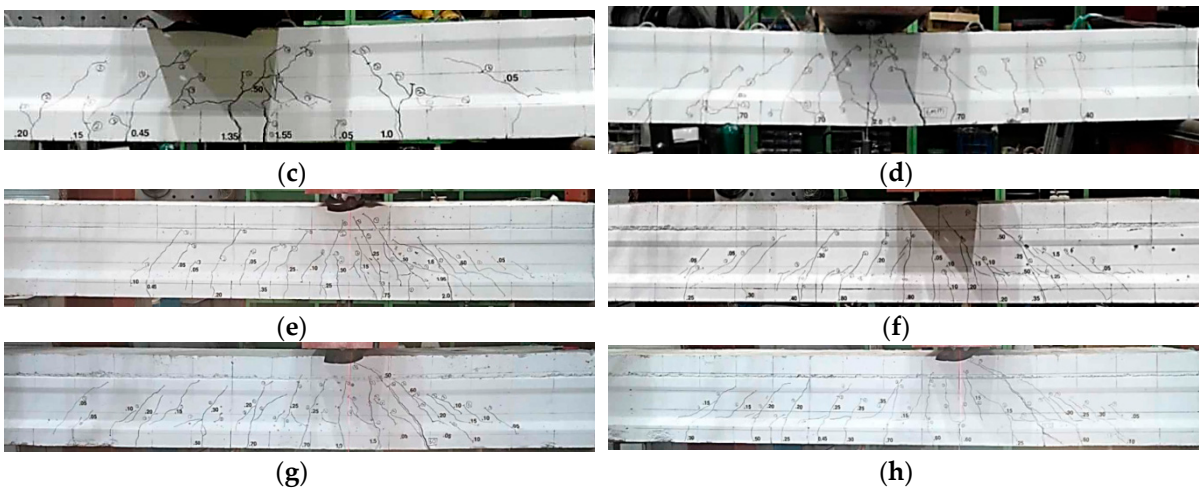

Figure 6. Crack patterns of specimens at failure. (**a**) US30 specimen. (**b**) US90 specimen. (**c**) US60a specimen. (**d**) US60b specimen. (**e**) CS30 specimen. (**f**) CSS90 specimen. (**g**) CSS30 specimen. (**h**) CSS90 specimen.

The composite slab specimens (CS series) showed similar initial cracking loads, ranging from 142 to 156 kN and flexural-shear cracks occurred at a load of about 190 to 205 kN. Unlike the US specimens, the CS specimens did not show a significant reduction in stiffness even after the occurrence of cracks and underwent failure as the critical crack width gradually increased without an abrupt reduction in load even after reaching the maximum load. The CS30 and CS90 specimens exhibited the maximum loads of 394 kN and 404 kN, respectively and the maximum loads of the CSS30 and CSS90 specimens, which had much more shear reinforcement, were 440 kN and 441 kN, respectively. For the composite specimens, there was almost no difference in strength between the specimens according to the inclination angle of the tapered cross section. This is because as the topping concrete is placed, the change of sectional area in the vicinity of the tapered cross section is smaller than that of the US specimens. As shown in Figure 6e–h, no significant difference in crack patterns was observed between the CS specimens. However, as shown in Figure 5, the CS90 and CSS90 specimens with a 1.57 rad (90°) inclination angle were found to have smaller deformation capacities after the maximum load than those of the CS30 and CSS30 specimens with a 0.52 rad (30°) inclination angle.

3.2. Measured Strains from Reinforcement

Figures 7 and 8 show strains measured in the US and CS specimens. Note that some gauges were damaged and failed to provide measurement values. In the graphs, "Compression," "Tension" and "Stirrup" represent the strain measured from gauges attached to the prestressing strands, longitudinal tensile reinforcement and shear reinforcement, respectively, while the gauge numbers signify the section locations shown in Figure 4c,d.

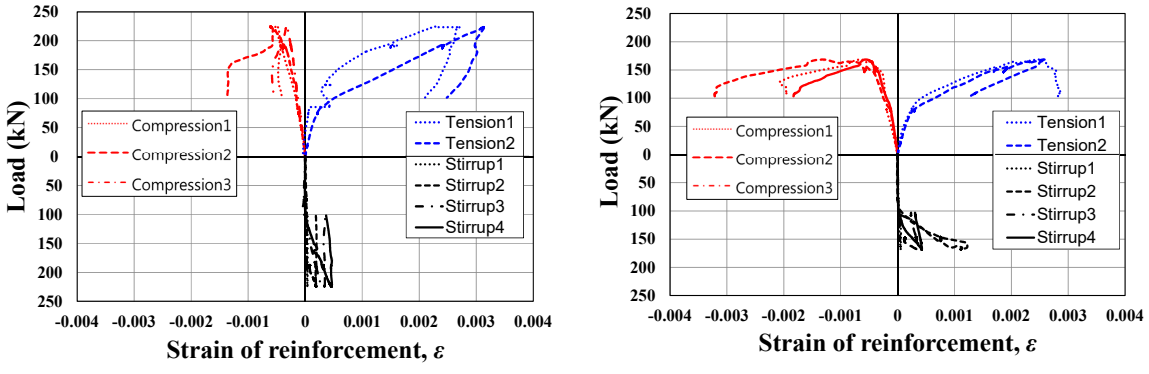

(**a**) (**b**)

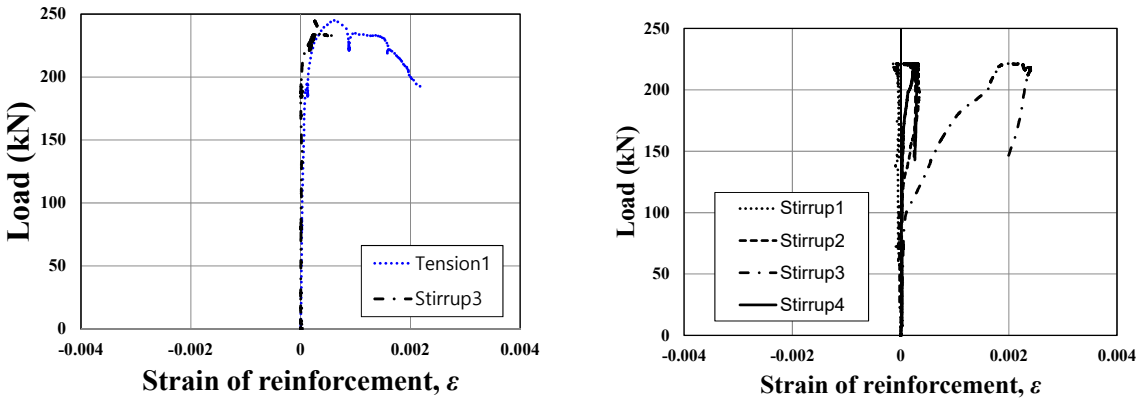

Figure 7. Strain behaviour of reinforcement in US specimens. (**a**) US30 specimen. (**b**) US90 specimen. (**c**) US60a specimen. (**d**) US60b specimen.

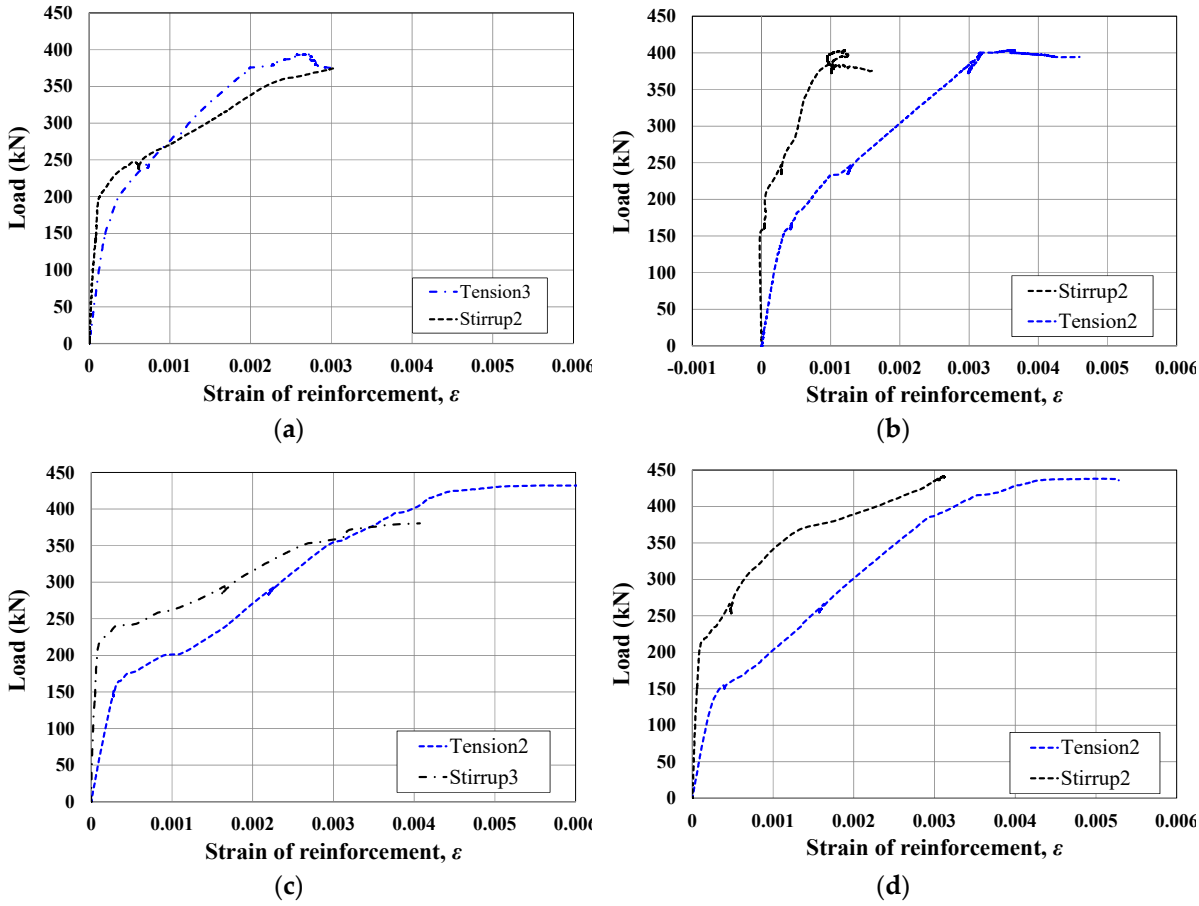

Figure 8. Strain behaviour of reinforcement in CS specimens. (**a**) CS30 specimen. (**b**) CS90 specimen. (**c**) CSS30 specimen. (**d**) CSS90 specimen.

As shown in Figure 7, the strain of shear reinforcement was considerably small in the US specimens, except for the US60b specimen and the strain of flexural tensile reinforcement increased greatly with the increasing loads. In particular, Figure 7b shows that the compressive strain of the upper strand was large enough to cause concrete crushing in the US90 specimen and the crushing failure of the concrete in the compression side occurred as shown in Figure 6b. In the case of the US60b specimen, only the strain of the shear reinforcement was measured due to the damage of the gauges and shear reinforcement located near the tapered cross section showed a larger strain than the yield strain.

Figure 8 shows the strains of the longitudinal tensile reinforcement and shear reinforcement, which are the largest strains among those measured from the CS specimens. Unlike in the US specimens, the strains measured from both the shear reinforcement and the flexural tensile reinforcement were greater than the yield strain in the CS specimens, except for a stirrup strain in the CS90 specimen. This suggests that the shear reinforcement effectively contributed to the shear resistance in the OPS with topping concrete.

4. Analysis for Design

4.1. Finite-Element Analysis Considering the Inclination Angle of the Tapered Cross Section

As observed in the test results, the shear performance of OPS is greatly influenced by the stress concentration that occurs near the tapered cross section and thus a detailed examination on the inclination angle of the tapered cross section is required [10]. In this regard, this study used a finite-element analysis (FEA) to investigate the effect of the inclination angle of the tapered cross section on the stress distribution in the OPS member. The finite-element analysis was performed using ABAQUS/CAE, a general-purpose analysis program [12] and it was aimed at comparing the stress distribution patterns according to the inclination angle of the tapered cross section rather than evaluating the performance of the members.

Figure 9 shows the finite-element analysis models for OPS. Only half of the member span was modelled using symmetric conditions [13]. As shown in Figure 9a, the concrete was modelled with solid elements and the prestressing strands and reinforcement were modelled with truss elements. The reinforcement materials were considered as being perfectly bonded with concrete. As shown in Figure 9b, Collins model and damaged plasticity model [12,14] were applied for the compressive and tensile behaviours of concrete and bilinear model and Ramberg-Osgood model [15–17] were applied to the reinforcement and prestressing strands, respectively. The material properties obtained from the experiments are summarized in Table 1. The proper mesh size was determined considering the mesh sensitivity and analysis efficiency and they were 50 mm and 140 mm for PC unit and topping parts, respectively, where the number of mesh elements was 25,729 and 1183, respectively. The concrete section was modelled by linear tetrahedral 3D solid elements (type C3D4) and the reinforcing bars were modelled by two-node 3D truss elements (type T3D2) [12,18]. The boundaries were modelled to simulate the simply supported conditions.

As shown in Figure 9c, the horizontal projection length of the slope (A) and the radius of the curve at the tapered cross section in the lower surface of the top flange (B) were set as the main analysis variables and the analysis for each variable was conducted on the cases shown in Table 2. The composite slab members (FEA2 series) were modelled with careful considerations on the characteristics of the contact surface between the PC slab unit and the topping concrete. In the production of the OPS, the surface is roughened on the upper part of the PC slab unit and the shear reinforcement to be placed in the member serves as a horizontal shear connector after the topping concrete composite. Therefore, the horizontal shear strength at the interface between the PC slab unit and the topping concrete can be estimated to be higher than 0.56MPa, which is the minimum horizontal shear strength presented in the ACI318-14 code [11]. In addition, no damage was observed at the interface between the PC slab unit and the topping concrete, even in the crack patterns shown in Figure 6. Therefore, in this study, 0.56 MPa and 0.6 were used for the cohesion (c) and the friction coefficient (μ), respectively, which are the interfacial contact characteristic between the PC slab unit and topping concrete [11].

Table 2. Variables for finite element analysis.

PC Slab Unit Case	A * (mm)	B * (mm)	Angle of Inclined Section (rad)	Composite Slab Case	A * (mm)	B * (mm)	Angle of Inclined Section (degree, °)
FEA1-1	200	200	0.983 (56.3°)	FEA2-1	200	200	0.983 (56.3°)
FEA1-2	250	200	0.876 (50.2°)	FEA2-2	250	200	0.876 (50.2°)

FEA1-3	400	200	0.644 (36.9°)	FEA2-3	400	200	0.644 (36.9°)
FEA1-4	250	150	0.876 (50.2°)	FEA2-4	250	150	0.876 (50.2°)
FEA1-5	400	150	0.644 (36.9°)	FEA2-5	400	150	0.644 (36.9°)

* refer to Figure 9c.

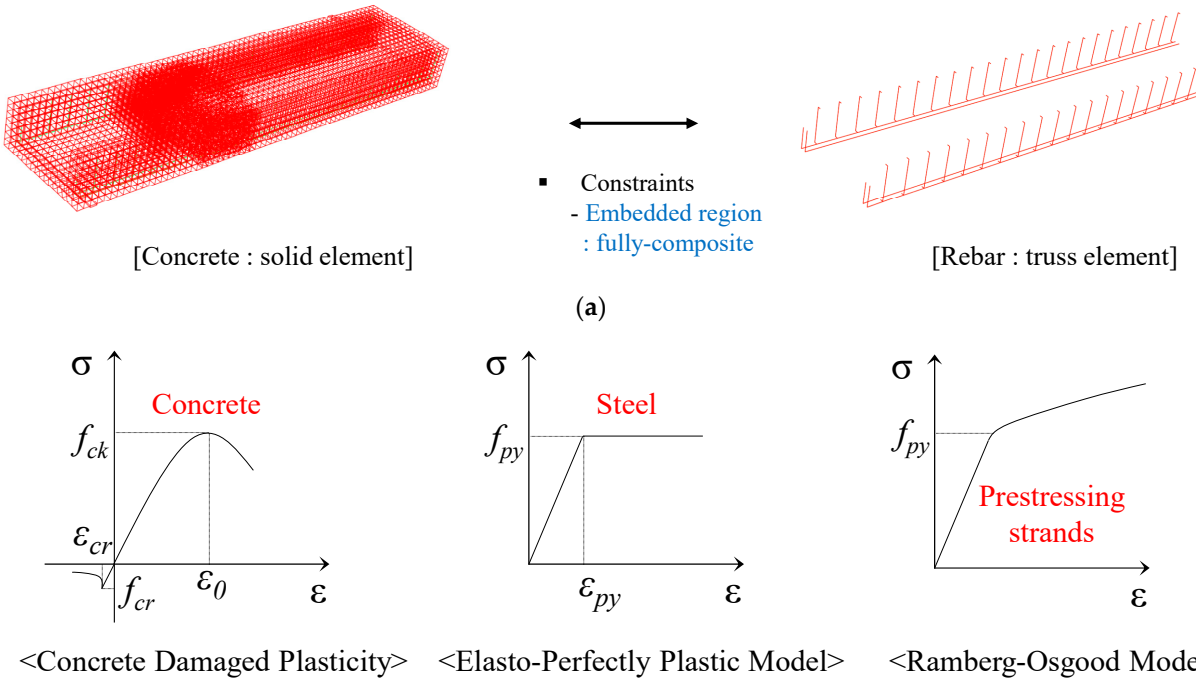

Figure 9. Finite element analysis model. (**a**) Interaction condition. (**b**) Material models. (**c**) Tapered cross section.

Figure 10a shows the analysis results on the FEA1 series, which are PC slab units without topping concrete. The cracked area, where the shear stress (v) is greater than the shear cracking strength (v_{cr}), was marked in a grey contour. In this case, when the shear cracking strength (v_{cr}), $0.33\sqrt{f_c'}$ is used [14] and 46.9MPa is applied as the concrete compressive strength (f_c') of the PC slab unit, v_{cr} is calculated to be 2.26 MPa. It can be confirmed from the analysis results that the stress is concentrated on the member end rib located at the support and on the web in the vicinity where the tapered cross section is formed. Figure 10b,c shows the analysis results on FEA 1-1 to 1-5 members according to variables A and B, respectively, where all analysis results are shown under the same deflection conditions. As shown in Figure 10b,c, the stress concentration tends to be mitigated as the inclination angle of the tapered cross section in the PC slab unit becomes smaller and the curvature of the curve at the tapered cross section in the lower surface of the top flange

becomes smaller. As mentioned in Section 3.1, the US90 specimen with an inclination angle of 1.57 rad (90°) underwent premature failure along with damages due to the stress concentration.

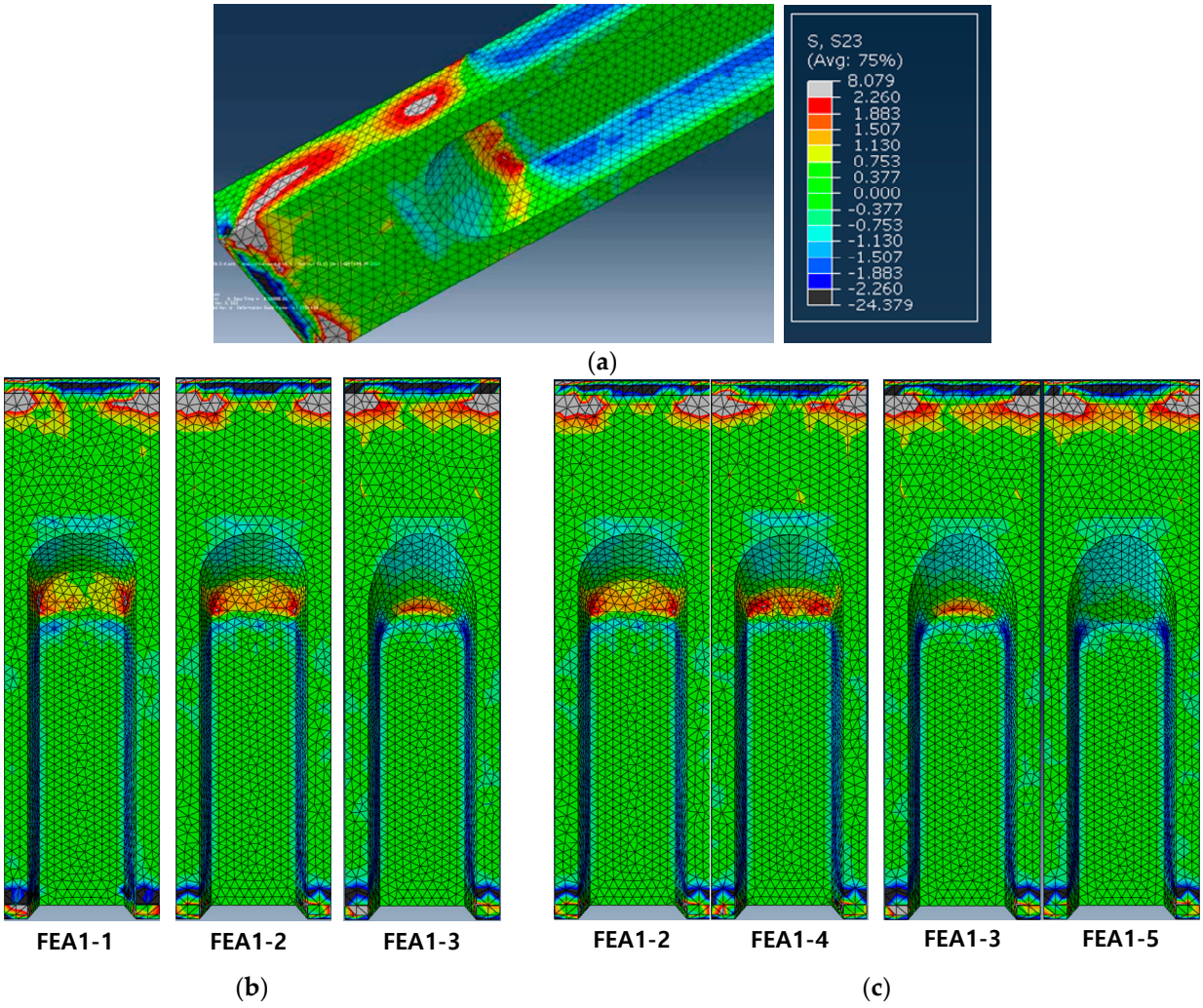

Figure 10. FEA results on PC slab units. (**a**) Shear stress distribution. (**b**) Shear stress distribution according to variable A. (**c**) Shear stress distribution according to variable B.

As shown in Figure 11, the finite-element analysis results on composite slabs (FEA2 series) also confirmed the mitigation of stress concentration with a smaller inclination angle of the tapered cross section and with a smaller curvature of the curve at the tapered cross section in the lower surface of the top flange, which were the same as in the FEA1 series. Therefore, the analysis and test results showed that, in order to alleviate the stress concentration occurring at the tapered cross section, it is desirable that the inclination angle of the tapered cross section should be less than 1.05 rad (60°) and the curvature of the curve at the tapered cross section in the lower surface of the top flange be as small as possible in the design step of OPS.

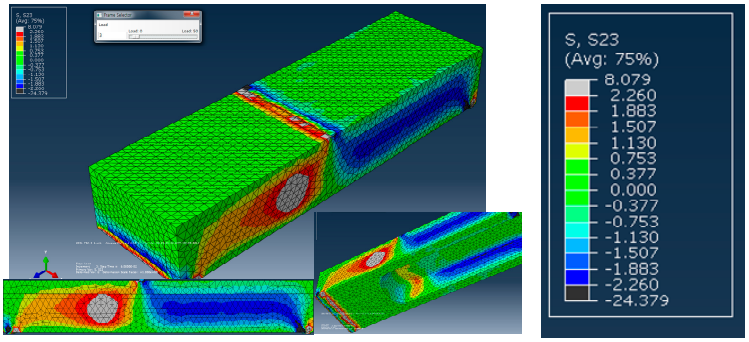

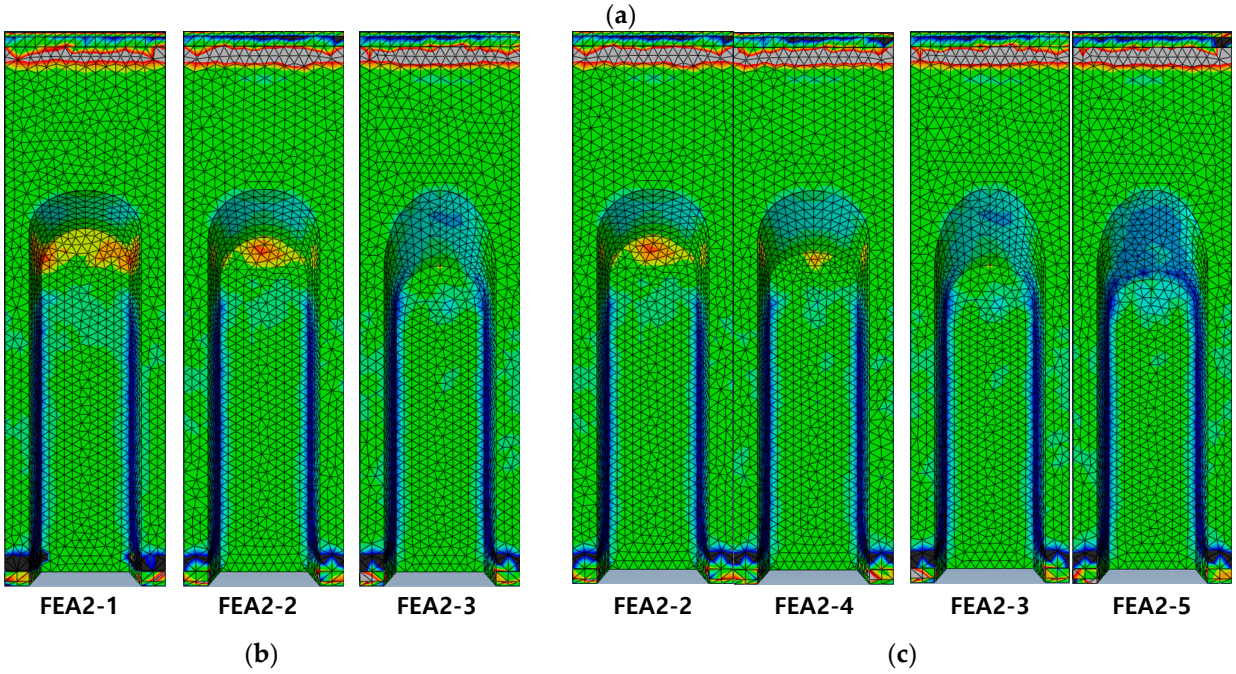

Figure 11. FEA results on composite slabs. (**a**) Shear stress distribution. (**b**) Shear stress distribution according to variable A. (**c**) Shear stress distribution according to variable B.

4.2. Suggestion for Estimating Shear Strength of OPS

In this study, the shear strengths of the specimens were evaluated using the shear design equations in ACI318-14 [11], as shown in Table 3. The prestressing strands placed in the OPS specimen have a straight profile and thus the vertical component of effective prestress (V_p) in the web shear strength of concrete (V_{cw}) is zero. The actual inclined crack angles measured from the test specimens were used for shear crack angles (β). In addition, since the location of critical shear cracks occurred in the specimens was not within the transfer length region, the effective stress (f_{pe}) was used to calculate the compressive stress at the centroid of the cross section after prestress release (f_{pc}) and the PC slab unit and topping concrete were considered to be fully composite based on the experimental observations. In the calculation of the shear strengths of the composite slab specimens, the compressive strength of the topping concrete rather than that of the PC slab unit was applied conservatively, as in most practical application cases. In addition, the test results were analysed in detail using the modified compression-field theory (MCFT) [19–22], which is a shear analysis model with proven accuracy and the code equations.

Table 3. Code equations for estimating shear strength of OPS [11].

Type	Code Equation*
Web shear strength of concrete	$V_{cw} = \left(0.29\sqrt{f_c'} + 0.3f_{pc}\right)b_w d_p + V_p$
Shear contribution of transverse reinforcement	$V_s = \frac{A_v f_y d}{s}\left(\sin\alpha\cot\beta + \cos\alpha\right)$

* Note: A_v = sectional area of stirrup (mm²); b_w = web width (mm); d_p = depth of prestressing strands (mm); d = effective depth of reinforcement (mm); f_c' = compressive strength of concrete (MPa); f_{pc} = compressive stress at centroid of cross section after prestress release (MPa); f_y = yield strength of transverse reinforcement (MPa); s = stirrup spacing (mm);

V_p = vertical component of effective prestress (N); α = angle of inclined stirrup (rad); β = angle of inclined shear crack (rad).

Table 4 and Figure 12 compare the shear strength test results (V_u) and analysis results (V_n). The ACI 318-14 code showed a tendency to overestimate the shear strengths of the US specimens, which are PC slab units. On the other hand, the MCFT provided a relatively approximate evaluation on the shear strengths of the US specimens, except for the US90 specimen, in which the inclination angle of the tapered cross section is 90°. Since the shear reinforcement placed in the OPS unit has a short embedment length and a stirrup hook at the top protrudes before the topping concrete is placed, as shown in Figure 3, the reinforcement may not develop up to its yield stress even if the shear cracks penetrate through the stirrups. This can be confirmed from the results of the shear reinforcement strain measurements shown in Figure 7. Therefore, the shear strengths of the US specimens represented as "Proposal" in Figure 12a were calculated by taking into account only the contribution of concrete (V_{cw}), excluding the contribution of shear reinforcement (V_s). This method provided a very accurate evaluation on the shear strengths of the PC slab unit specimens, except for the US90 specimen. It should again be noted that the US90 specimen underwent premature failure due to excessive stress concentration on the region of the tapered cross section.

Table 4. Comparison of test and analysis results.

Specimen	Critical Crack Angle (degree)	Compressive Strength of Concrete (MPa)	Spacing of Shear Reinforcement (mm)	Test Results, V_u (kN)	Analysis Results, V_n (kN)		
					ACI 318	MCFT	Proposal
US30	32.0	55.0	400	151.8	189.1	161.3	149.0
US60a	90.0	46.9	400	167.5	188.7	136.5	144.1
US60b	60.3	46.9	400	149.7	188.7	136.5	144.1
US90	36.9	55.0	400	113.9	189.1	149.3	149.0
CS30	54.5	49.0	400	266.2	276.2	239.5	260.8
CS90	56.3	49.0	400	272.7	273.2	239.5	260.8
CSS30	57.5	49.0	300	297.1	303.2	275.7	290.4
CSS90	56.3	49.0	300	298.1	305.4	275.7	290.4

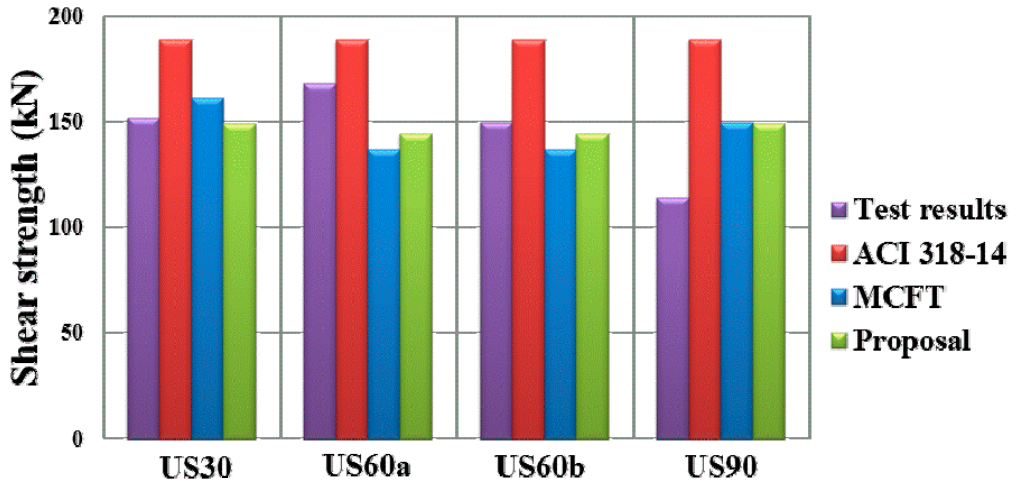

(**a**)

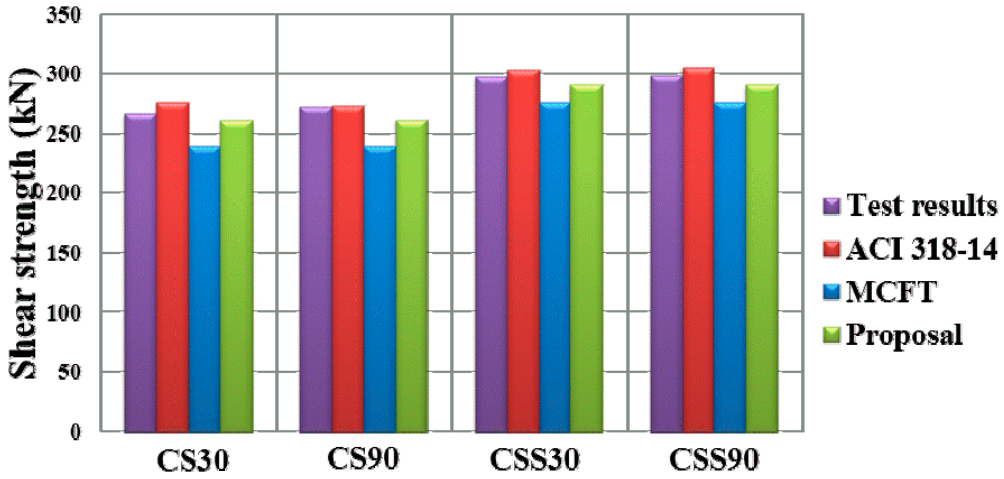

(**b**)

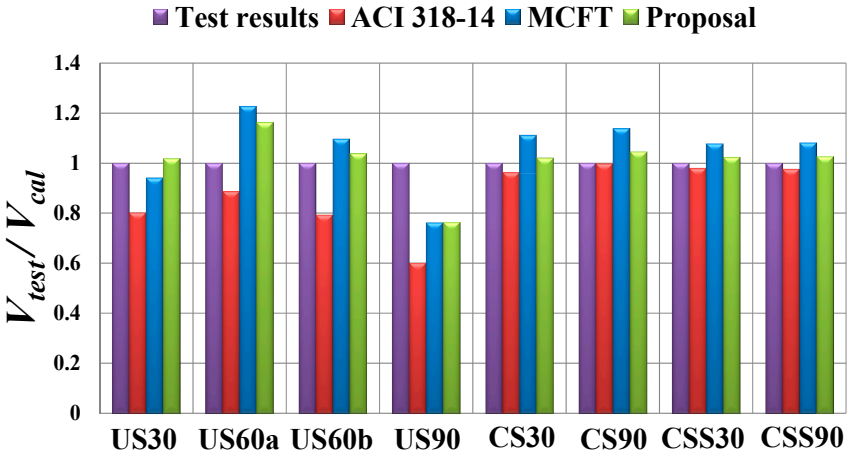

(**c**)

Figure 12. Shear strength evaluation results. (**a**) PC slab unit specimens. (**b**) Composite slab specimens. (c) Variations between analysis and test results.

In the case of the CS specimens with topping concrete, the MCFT provided conservative estimations on the shear strengths of the test specimens. On the other hand, the ACI 318-14 code showed a tendency to overestimate the test results to some extent but provided relatively accurate shear strengths when compared to the US specimens. As shown in Table 4, the critical shear crack angles observed in the CS specimens ranged from 0.93 rad (53.5°) to 1.00 rad (57.5°), which are considerably larger than the shear crack angles generated in ordinary reinforced concrete and prestressed concrete members [1,11]. The reason why the shear crack is formed at such a high angle is that the stress concentration phenomenon is greatly influenced by the inclination angle of the tapered cross section. In the case of having a steep angle of the tapered cross section as in the US90 specimen, therefore a premature failure can occur because of excessive stress concentration. Hence it is necessary to form the angle of the tapered cross section as low as possible and there is a need to assume that the crack angle (β) is larger than that of the typical slab member for safe shear design for OPS. Accordingly, $\beta = 1.05$ rad (60°) was applied in the calculation of shear strengths for "Proposal" shown in Figure 12b and this method was found to provide a very accurate evaluation on the shear strengths of the CS specimens. Therefore, if the shear strength is calculated by considering only the contribution of concrete (V_{cw}) in the construction phase and if the contribution

of shear reinforcement (V_s) is estimated under the assumption that the crack angle (β) is 1.05 rad (60º) after the topping concrete is placed, then adequate safety can be ensured in the shear design of the OPS member.

5. Conclusions

In this study, an experimental investigation was carried out to examine the shear performance of the optimized-section precast slab (OPS). The effect of the shape of the tapered cross section on the stress concentration was analysed by means of a finite-element analysis. In addition, a shear-design method for the OPS member, which ensures adequate safety was proposed based on a detailed comparative analysis between ACI318-14 and the test results. The following conclusions were obtained from this study.

1. In the PC slab unit specimen where the inclination angle of the tapered cross section was 1.57 rad (90°), premature failure occurred because excessive stress was concentrated at the region of the tapered cross section. On the other hand, the inclination angle of the tapered cross section did not much influence the shear strength of the member in the composite slab specimen with topping concrete. This is because the composite slab specimens have a smaller change in sectional area near the tapered cross section due to the placement of topping concrete, as compared to the US specimens.
2. The finite-element analysis results showed that as the inclination angle of the tapered cross section and the curvature of the curve at the tapered cross section in the lower surface of the top flange became smaller, the stress concentration decreased. The shear tests also found that the PC slab unit specimens with an inclination angle of less than 1.05 rad (60°) had very similar shear strengths. Therefore, it is desirable that the tapered cross section be configured to have an inclination angle of less than 1.05 rad (60°) in the design of the OPS.
3. The shear reinforcement placed in the PC slab unit specimens did not yield even at the ultimate strength and thus the specimens showed lower strengths than those from the current code equations. Therefore, the shear contribution of shear reinforcement (V_s) should be excluded and only the contribution of concrete (V_{cw}) should be considered in the shear design of the PC slab unit members. This estimation method not only revealed that the shear strengths of the specimens are on the safe side but also provided a very accurate evaluation of them.
4. The shear crack angle observed in the composite slab specimens with topping concrete was about 0.96 rad (55º), which is steeper than those in typical reinforced concrete and prestressed concrete members. Therefore, it is expected that a proper safety can be ensured in the shear design of the composite OPS members when the crack angle (β) of 1.05 rad (60º) is used to calculate the contribution of shear reinforcement (V_s).

Author Contributions: Original draft manuscript, H.J.; Validation, S.-J.H. and H.-E.J.; Investigation, H.-C.C. and Y.-H.O.; Supervision and Review Writing, K.S.K.

Acknowledges: This research was supported by Basic Science Research Program through the National Research Foundation of Korea (NRF) funded by the Ministry of Education (2016R1D1A3B03932214).

Conflicts of Interest: The authors declare no conflict of interest.

References

1. Ju, H.; Han, S.J.; Choi, I.S.; Choi, S.; Park, M.K.; Kim, K.S. Experimental Study on an Optimized-Section Precast Slab with Structural Aesthetics. *Appl. Sci.* **2018**, *8*, 1234, doi:10.3390/app8081234.
2. Korea Environmental Industry and Technology Institute. *Korea LCI Database Information Network*; Korea Environmental Industry and Technology Institute: Seoul, Korea, 2013.
3. Choi, I.S. Structural Performance of Precast Slab with Esthetics and Optimized Section for Positive and Negative Moment. Ph.D. Thesis, Inha University, Incheon, Korea, 2016.

4. Elliot, K.S.; Colin, K.J. *Multi-Storey Precast Concrete Framed Structures*, 2nd ed.; Wiley Blackwell: Hoboken, NJ, USA, 2013.
5. Mejia-McMaster, J.C.; Park, R. Test on special reinforcement for the end support of hollow-core slabs. *PCI J.* **1994**, *39*, 90–105, doi:10.15554/pcij.09011994.90.105.
6. Gere, J.M.; Goodno, B.J. *Mechanics of Materials*, 8th ed.; Cenage Learning: Boston, MA, USA, 2012.
7. Rosenthal I. Full scale test of continuous prestressed hollow-core slab. *PCI J.* **1978**, *23*, 74–81, doi:10.15554/pcij.05011978.74.81.
8. Tan, K.H.; Zheng, L.X.; Paramasivam, P. Designing hollow-core slabs for continuity. *PCI J.* **1996**, *41*, 82–91, doi:10.15554/pcij.05011978.74.81.
9. Yang, L. Design of Prestressed Hollow-Core Slabs with Reference to Web-Shear Failure. *J. Struct. Eng.* **1994**, *120*, 2675–2696, doi:10.1061/(asce)0733-9445(1994)120:9(2675).
10. Lee, D.H.; Park, M.K.; Oh, J.Y.; Kim, K.S.; Im, J.H.; Seo, S.Y. Web-shear Capacity of Prestressed Hollow-Core Slab Unit with Consideration on the Minimum Shear Reinforcement Requirement. *Comput. Concr.* **2014**, *14*, 211–231, doi:10.12989/cac.2014.14.3.211.
11. ACI Committee 318. *Building Code Requirements for Reinforced Concrete and Commentary (ACI 318-14)*; American Concrete Institute: Farmington Hills, MI, USA, 2014.
12. Hibbitt, H.; Karlsson, B.; Sorensen, P. *ABAQUS Analysis Users Manual*; Version 6.10; Dassault Systemes Simulia: Providence, RI, USA, 2011.
13. Smith, I.M.; Griffiths, D.V. *Programming the Finite Element Analysis*, 4th ed.; John Wiley and Sons, Ltd.: Hoboken, NJ, USA, 2004.
14. Collins, M.P.; Mitchell, D. *Prestressed Concrete Structures*; Prentice-Hall: Upper Saddle River, NJ, USA, 1991.
15. MacGregor, J.G.; Wight, J.K. *Reinforced Concrete Mechanics and Design*, 4th ed.; Prentice-Hall: Upper Saddle River, NJ, USA, 2006.
16. Mattock, A.H. Flexural strength of prestressed concrete sections by programmable calculator. *PCI J.* **1979**, *24*, 32–54, doi:10.15554/pcij.01011979.32.54.
17. Lee, D.H.; Oh, J.Y.; Kang, H.; Kim, K.S.; Kim, H.J.; Kim, H.Y. Structural Performance of Prestressed Composite Girders with Corrugated Steel Plate Webs. *J. Constr. Steel Res.* **2015**, *104*, 9–21, doi:10.1016/j.jcsr.2014.09.014.
18. Oh, J.Y.; Lee, D.H.; Cho, S.H.; Kang, H.; Cho, H.C.; Kim K.S. Flexural Behavior of Prestressed Steel-Concrete Composite Members with Discontinuous Webs. *Adv. Mater. Sci. Eng.* **2015**, *2015*, 278293, doi:10.1155/2015/278293.
19. Vecchio, F.J.; Collins, M.P. Modified Compression-Field Theory for Reinforced Concrete Elements Subjected to Shear. *ACI J. Proc.* **1986**, *83*, 219–231, doi:10.14359/10416.
20. Vecchio, F.J.; Collins, M.P. Predicting the Response of Reinforced Concrete Beams Subjected to Shear Using Modified Compression Field Theory. *ACI Struct. J.* **1988**, *85*, 258–268, doi:10.14359/2515.
21. Bentz, E.C.; Vecchio, F.J.; Collins, M.P. Simplified Modified Compression Field Theory for Calculating Shear Strength of Reinforced Concrete Elements. *ACI Struct. J.* **2006**, *103*, 614–624, doi:10.14359/16438.
22. Bentz, E.C. Sectional Analysis of Reinforced Concrete Members. Ph.D. Thesis, University of Toronto, Toronto, ON, Canada, 2000.